Event-triggered Add-on Safety for Connected and Automated Vehicles Using Road-side Network Infrastructure

Mohammad H. Mamduhi [*] **Ehsan Hashemi** [**]
John S. Baras [*,***] **Karl H. Johansson** [*]

[*] *Division of Decision and Control Systems, School of Electrical Engineering and Computer Science, Royal Institute of Technology, Stockholm, Sweden (e-mail: {mamduhi,baras,kallej}@kth.se).*
[**] *Mechanical and Mechatronics Engineering Department, University of Waterloo, ON, Canada (e-mail: ehashemi@uwaterloo.ca)*
[***] *Department of Electrical and Computer Engineering, University of Maryland College Park, MD, USA (e-mail: baras@umd.edu)*

Abstract:
This paper proposes an event-triggered add-on safety mechanism to adjust the control parameters for timely braking in a networked vehicular system while maintaining maneuverability. Passenger vehicle maneuverability is significantly affected by the combined slip friction effect, in which larger longitudinal tire slips result in considerable drop in lateral tire forces. This is of higher importance when unexpected dangerous situations occur on the road and immediate actions, such as braking, need to be taken to avoid collision. Harsh braking can lead to high-slip and loss of maneuverability; hence, timely braking is essential to reduce high-slip scenarios. In addition to the vehicles own active safety systems, the proposed event-triggered add-on safety is activated upon being informed about dangers by the road-side infrastructure. The aim is to incorporate the add-on safety feature to adjust the automatic control parameters for smooth and timely braking such that a collision is avoided while vehicle's maneuverability is maintained. We study two different wireless technologies for communication between the infrastructure and the vehicles, the Long-Term Evolution (LTE) and the fifth generation (5G) schemes. The safety advantages of the proposed framework is validated through high-fidelity software simulations.

Keywords: Connected vehicles, V2I-I2V communication, Add-on safety, 5G network slicing.

1. INTRODUCTION

The potential to enable fast and reconfigurable mechanisms for increasingly prevalent Automated Driving Systems (ADS), cooperative vehicles, and advanced driver-assistance systems (ADAS) underscores the critical need to develop more reliable safety mechanisms within the distributed-system framework for intelligent transportation systems. The functionality of mentioned mechanisms has gradually shifted from stabilization of vehicle/wheel dynamics to taking control in emergency cases and guidance control (Bengler et al. (2014); Linsenmayer et al. (2017)). Connected vehicles with partially or conditionally automated driving features (known as Level 3 to Level 4 in vehicles autonomy) not only utilize several ADS control systems, such as differential braking, torque vectoring, and active steering, but also can benefit from shared information over network nodes and infrastructure to have more proactive and reliable lateral/longitudinal stability control and to enable dramatic improvements in fuel efficiency, see Lu et al. (2014); Chang and et al. (2015); Hung et al. (2019). Differential braking strategies in vehicle active safety systems are capable of stabilizing the vehicle not only by expanding the safe operating envelope due to optimal speed reduction, but through generating corrective yaw moment to enhance yaw tracking performance based on the request from the path planner or the driver. Having information about road emergency cases significantly improves performance of the braking actuation due to the fact that local vehicle controllers apply corrective longitudinal forces less aggressively, leading to less longitudinal slip (Ito et al. (2018)). This results in less lateral tire force drop, thus, increases maneuverability and capability of the automated driving system (or the driver) in obstacle avoidance, sudden path changes, and speed reduction.

New communication technologies such as 5G, provide fast, flexible and application-oriented network services that can be adjusted according to user-demands or criticality of the situation (Molina and Jacob (2018)). Features such as network slicing, virtualization, and software-defined networking can be utilized to enhance the coordination of information in time-sensitive applications, such as smart transportation. Specifically for safe connected vehicles, communication with road-side network infrastructure, in the form of Vehicle-to-Infrastructure (V2I) and Infrastructure-to-Vehicle (I2V), can lead to significant improvement of safety margins through transmission of critical information about the road situation (Campolo et al. (2017)). To the best of our knowledge, event-triggered add-on safety frameworks (to be utilized on existing low-level traction and stability control systems) has not been provided in the literature.

An interesting feature that can be utilized is virtual network slicing. Operating on the same physical hardware, virtual network slices generally consist of independent sets of software functionalities to support the service requirements for specific applications, see Lucena et al. (2017). These functionalities include bandwidth, speed, coverage, privacy and connectivity that can be independently implemented and optimized to satisfy particular user demands.

We propose an event-based add-on safety mechanism to enhance vehicle controllability at the events of occurring unexpected dangers on the road. Upon occurrence of a danger, the vehicle detecting it transmits a warning signal to the road-side infrastructure to be broadcasted to other vehicles that might not yet have detected the danger. Depending on how fast the communication is performed, this may result in a faster notice of the imminent danger for those vehicles that do not directly face it. Arrival of the warning signal triggers the add-on safety mechanism that, together with ADS, control the vehicle such that the danger is safely avoided with smooth braking. The communication technology at the road-side infrastructure determines the quality of data coordination. We study two communication schemes, LTE and 5G, as the supporting network available at base stations and evaluate their performance in safety augmentation of the vehicles.

In the rest of this paper, the problem scenario is described in Sec. 2. The proposed add-on safety mechanism and the communication schemes are discussed in Sec. 3. Performance analyses are provided in Sec. 4, and simulation results are shown in Sec. 5, and Sec. 6 concludes the paper.

2. SYSTEM MODEL AND PROBLEM SCENARIO

2.1 Vehicular network model

In a vehicular network with second-order consensus realization, the kinematic description of each vehicle i yields $\dot{p}^i(t) = v^{xi}(t)$, $\dot{v}^{xi}(t) = u^i(t) + \varrho^i(t)$, where p^i, v^{xi} are the differences between the desired vehicle longitudinal position/speed trajectories (with a common constant speed v_d^{xi}) and the measured/absolute ones $\bar{p}^i, \bar{v}^{xi}$ and $\varrho^i(t)$ is a zero-mean Gaussian uncertainty uncorrelated across the connected vehicle. The effect of vehicle yaw rate on the longitudinal kinematics is ignored. Thus, the measured longitudinal acceleration a^{xi} can be expressed as the time derivative of longitudinal speed $\dot{\bar{v}}^{xi}$. The desired position for each vehicle is defined by $p_d^i = v_d^{xi}t + s_i$, where v_d^{xi} is the common constant speed and s_i is a given desired spacing. The vehicle speed v^{xi} can be measured by GPS or estimated by using inertial measurement unit (IMU) and wheel encoders (Selmanaj et al. (2017)). Inspired by the work in (Öncü et al. (2014)) and (Tegling, 2018, Ch. 4), and having access to position and velocity errors, we define the control input for each vehicle i at time t, with the set of neighboring vehicles denoted by $\mathcal{N}_i$, as

$$u^i(t) = -\sum_{j\in\mathcal{N}_i} \bar{c}_{ij}^p (p^i(t) - p^j(t)) - \sum_{j\in\mathcal{N}_i} \bar{c}_{ij}^v (v^{xi}(t) - v^{xj}(t)) - c_0^p p^i(t) - c_0^v v^{xi}(t), \quad (1)$$

where $\bar{c}_{ij}^p$ and $\bar{c}_{ij}^v$ represent constant relative position and velocity gains in the conventional vehicular formation framework, and c_0^p and c_0^v denote the constant gains to adjust the position and velocity of vehicle i w.r.t. its desired

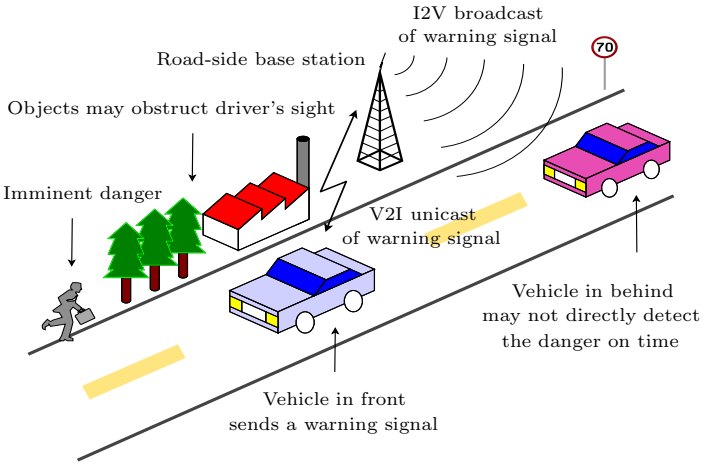

Fig. 1. Front vehicle detects an imminent danger and informs the following vehicles via sending a warning signal using V2I-I2V with the road-side base station.

trajectories. Combining the kinematics of all vehicles and the control input, the closed-loop model of the vehicular network can be written as $\dot{x} = \bar{A}x + \bar{B}\boldsymbol{\varrho}$, with the augmented state vector $x \triangleq [p, v] = [p^1, p^2, \ldots, v^{x1}, v^{x2}, \ldots]^\top$, and

$$\bar{A} = \begin{bmatrix} \mathbf{0} & \mathbf{I} \\ -c_0^p\mathbf{I} - \mathcal{L}_{c^p} & -c_0^v\mathbf{I} - \mathcal{L}_{c^v} \end{bmatrix}, \ \bar{B} = \begin{bmatrix} \mathbf{0} \\ \mathbf{I} \end{bmatrix}, \quad (2)$$

in which $\mathcal{L}_{c^p}, \mathcal{L}_{c^v}$ are position and velocity weighted graph Laplacian matrices with weights $\bar{c}_{ij}^p$ and $\bar{c}_{ij}^v$, respectively. Since communication operates in time-slotted fashion, we consider the discrete-time model of the vehicular network system, which can be described as $x(k+1) = Ax(k) + B\boldsymbol{\varrho}(k)$ with state and input matrices A, B obtained by the zero-order hold, i.e., $A = e^{\bar{A}(t)T_s}$ and $B = \int_0^{T_s} e^{\bar{A}(t)\tau}\bar{B}(t)d\tau$, with T_s denoting the sampling time. Hence, the dynamics of the vehicle at time-step $k \in \mathbb{N}\cup\{0\}$ is the sample of its continuous model at time kT_s, and the next sample time $k+1$ equals $kT_s + T_s$. We assume T_s is small enough, and all vehicles of the network have identical sampling times.

2.2 Problem scenario

We model V2I-I2V communication via the road-side base stations (BS) to warn the neighboring vehicles about an existing danger. We consider situations that vehicles do not expect a danger and the vehicles not directly facing the danger may not be capable of detecting it in time, e.g., if a pedestrian suddenly jumps onto the vehicle lane (see Fig. 1). In these situations, the vehicles behind can be informed about the imminent danger by the vehicle facing it using the road-side BS. This information can lead to significant enhancement of braking and vehicle handling performances as it serves the vehicle (or automated driving) stability programs to generate required longitudinal forces less aggressively, which leads to less longitudinal and lateral tire force drop. We refer to an unexpected danger situation and the time of its occurrence as *danger* and *danger time*, respectively. Since the described on-road dangers occur sporadically with uncorrelated random frequency, we intuitively assume that the probability of occurring a danger is independent of the previous ones.

Define by t_n the n^{th} danger time. The set of danger times up to an arbitrary time-step k is then $\mathcal{D}_k \triangleq \{t_1, \ldots, t_n\}$, $t_n \le k$, where $t_1, \ldots, t_n$ are statistically uncorrelated.

Each vehicle is assumed to be equipped with an add-on safety mechanism that is activated upon receiving a warning signal about an imminent danger. The vehicle detecting a danger immediately transmits a warning signal to the infrastructure to be broadcasted to the vehicles in behind. Those receiving the warning signal will activate their add-on safety mechanism and adjust their control actions accordingly to avoid collision or loss of maneuverability. We define the binary-valued triggering variable θ_k^i, corresponding to the vehicle i at time-step k, as follows

$$\theta_k^i = \begin{cases} 1, & \text{if } \exists\, t_n \in \mathcal{D}_k \text{ such that: } t_n \in (k-1, k], \\ 0, & \text{if } \forall\, t_n \in \mathcal{D}_k : \ \ t_n \leq k-1, \end{cases} \tag{3}$$

where $\theta_k^i = 1$ activates the add-on safety mechanism at time-step k and it remains activated until the vehicle is at complete standstill. Incorporating the event-triggered variable θ_k^i, we introduce the additive gains Δc_i^p and Δc_i^v as add-on safety features to adjust the control input. The new time-varying control gains then are realized as $\bar{c}_{ij}^p(k) = \bar{c}_{ij}^p + \theta_k^i \Delta c_i^p$ and $\bar{c}_{ij}^v(k) = \bar{c}_{ij}^v + \theta_k^i \Delta c_i^v$, affecting the closed-loop behavior in $x(k+1) = A(k)x(k) + B(k)\boldsymbol{\varrho}(k)$.

The discrete-time control input u_k^i for vehicle i with active add-on safety mechanism, i.e. if $\theta_k^i = 1$, can be stated as

$$\begin{aligned} u_k^i = &- \sum_{j \in \mathcal{N}_i} (\bar{c}_{ij}^p + \theta_k^i \Delta c_i^p)(p_k^i - p_k^j) \\ &- \sum_{j \in \mathcal{N}_i} (\bar{c}_{ij}^v + \theta_k^i \Delta c_i^v)(v_k^{xi} - v_k^{xj}) - c_0^p p_k^i - c_0^v v_k^{xi}. \end{aligned} \tag{4}$$

The augmented control input vector $u_k \triangleq [u_k^1, u_k^2, \ldots]$ of the vehicular network at time-step k, can be expressed as

$$u_k = -\left[c_0^p \mathbf{I} + \bar{\mathcal{L}}_{c^p} \ \ c_0^v \mathbf{I} + \bar{\mathcal{L}}_{c^v}\right] x, \tag{5}$$

where, $\bar{\mathcal{L}}_{c^p}$ and $\bar{\mathcal{L}}_{c^v}$ are the position and velocity Laplacian matrices of the vehicular network weighted by the new gains $\bar{c}_{ij}^p + \theta_k^i \Delta c_i^p$ and $\bar{c}_{ij}^v + \theta_k^i \Delta c_i^v$, respectively.

Remark 1. In line with real technology, we assume that all vehicles in the network are equipped with Anti-lock Braking Systems (ABS), which prevents large slip ratios, thus, maintains lateral tire force capacities. ABS also keeps longitudinal forces around the saturation region, before which tire forces are linear. In fact, as we discuss it in Sec. 4, before the saturation region, it is convenient to consider a linear model for the slip ratio w.r.t the tire forces. One of main features of the developed control structure is that the control input could be adjusted by information on tire capacities in various vehicles having different low-level traction and ABS controllers.

3. VEHICLE COMMUNICATION MODEL

In case of detecting a danger by a vehicle, a warning signal is transmitted for the in-range road side BS. For technical correctness, we consider two assumptions: 1) for any vehicle there is always a road side BS in range so that the vehicle can communicate with, and 2) the task of hand over from one BS to the next is performed perfectly and instantaneously. Each BS is assumed to service a regular stationary traffic that is statistically independent from the traffic of warning signals. Warning signals are transmitted to the BS in unicast fashion, i.e. from a single network node (vehicle) to a designated target node (BS), and they arrive at the BS with a time delay, so called, uplink latency.

In the following, we first introduce the scenario without V2I-I2V communication and then discuss two wireless network technologies; non-scheduled queue-based Long Term Evolution (LTE) approach, and resource-aware 5G network for the V2I-I2V scenario. We further evaluate the effects of the described scenarios on vehicles' safety margins. For the comparison purposes, the constant gains $\bar{c}_{ij}^p$, $\bar{c}_{ij}^v$, c_0^p and c_0^v are assumed identical for all scenarios.

3.1 Vehicle control without V2I-I2V communication

Assume that if a road danger occurs, no warning signal is communicated via the road-side infrastructure. The V2V communication may exist and the following vehicle (denoted by index i) can receive the brake status of the front vehicle (denoted by index j), using the brake position sensors. Hence, vehicle i is informed of a change in brake status of vehicle j, if the brake of vehicle j is activated.

Driver Reaction Time (RT) is the temporal duration from the time instant the driver detects a danger until an action (braking) is executed. Characterizing RT is complicated because it is a function of many parameters such as driver's age, awareness, tiredness, eyesight, weather and visibility condition. Many real and simulator-driven tests are carried out to provide categorically acceptable average values of RT. A main categorization corresponds to the "unexpectedness" of the stimuli. It is reported in (Krauss and Olson (2015)) that for clearly-visible stimulus, about 85-95% of drivers have unanticipated RTs of about $1.5s$, while the minimum observed RT is on average not less than $0.75s$. In this paper, the aim is to show that even if a driver has a short RT, incorporating V2I-I2V communication can still improve vehicle safety. Hence, we select a relatively short RT of $0.7s$ for any driver on the road. The presented results remain valid for any longer driver RT. Having this, if a danger occurs in front of the vehicle j, the earliest the vehicle i detects it is when the driver of vehicle j activates the brake, i.e, after elapsing the RT. Assuming the ADAS of vehicle j reacts immediately, it takes on average $0.7s$ to execute braking from the time of detecting the danger.

3.2 Non-scheduled LTE-based V2I-I2V communication

Now we assume that warning signals are sent to a LTE road-side BS to be broadcasted to the neighboring vehicles. We model the communication technology at the BS as a time slotted channel with limited bandwidth, i.e., at each slot, only a finite number of transmission requests can be serviced. If there are more arrivals, they are queued based on the arrival time and transmissions occur when bandwidth is assigned. Hence, some requests are delivered to the recipients by queuing delay. We, moreover, assume that the BS is not capable of scheduling, hence, every data arriving at the BS, either the emergency warning signals or regular traffic, are queued in a simple first-in first-out (FIFO) buffer and data is discharged depending on the queue length and the assigned bandwidth (Fig. 2).

We denote the arrival and departure traffics at the BS at time-step k by $a_k \in \mathbb{Z}_{\geq 0}$ and $d_k \in \mathbb{Z}_{\geq 0}$, respectively. Therefore, if the queue has the length $\ell_k \in \mathbb{Z}_{\geq 0}$ at time-step k, the process ℓ_{k+1} has the following evolution

$$\ell_{k+1} = a_k + \max[\ell_k - d_k, 0], \quad \ell_0 = 0. \tag{6}$$

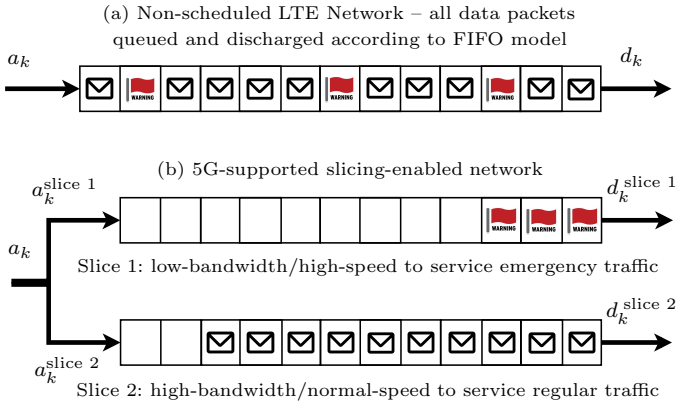

Fig. 2. (a) LTE non-scheduled and (b) 5G slicing-enabled BS serviceability. Red flags and envelopes depict the warning signals and regular traffic, respectively.

To avoid infinite delays, we assume that queues at BSs are rate stable, i.e., $\mathsf{P}\big[\lim_{t\to\infty}\frac{\ell_t}{t}=0\big]=1$, which holds if and only if ((Neely, 2010, Th. 2.4)) $\lim_{t\to\infty}\frac{1}{t}\sum_{\tau=0}^{t-1}[a_\tau-d_\tau]\leq 0$. Note that, rate stability is a time-averaged condition. Therefore, here might be time instances that the realized departure bandwidth cannot service all the arrived packets plus the ones already queued. Hence, data delivery would experience delays at finite number of instances.

We consider $M/M/1$ queues at the BSs which specifies that the arrival traffic at the BS follows the *Poisson* distribution and the service times are distributed *exponentially*. Compared to the scenario without V2I-I2V communication, here the following vehicle is informed about the existing danger subject to the uplink and downlink latency plus queuing service delay. We denote the uplink and downlink delays by τ_{ul} and τ_{dl}, respectively, where τ_{dl} is the time between a warning signal being broadcasted by the BS until it is received by the vehicles. Queuing delay is also denoted by τ_q, with the mean $0\leq\mathsf{E}[\tau_q]<1$ for pre-empty queues (Mamduhi et al. (2018)). Therefore, if a danger is detected by vehicle j at time-step k, the transmitted warning signal is received by the vehicle i at $k+\tau_{ul}+\tau_q+\tau_{dl}$. For technical convenience regarding the discretized model, the warning signal transmitted by the vehicle j at time-step k will be received by the vehicle i at time $k+r$, $r\in\mathbb{Z}_{\geq 0}$, where $rT_s\leq\tau_{ul}+\tau_q+\tau_{dl}<(r+1)T_s$.

3.3 5G-supported slicing-enabled V2I-I2V communication

Now assume that 5G-supported road-side BSs are in range. In accordance with the capabilities of 5G networks, we consider a simple service slicing mechanism available for the BSs facilitating a situation-aware serviceability. [1] Employing the network slicing scheme (see Fig. 2), the flagged warning signals are serviced via a specific network slice including a dedicated transmission link. Knowing that the dangers occur sporadically on the road while the warning signals need to be transmitted as fast as possible, the communication resources (bandwidth and latency) are assumed to be divided into one high-speed and low-bandwidth slice to support fast transmission of the emergency warning signals, and a regular-speed high-bandwidth slice for the transmission of regular traffic.

[1] For more information on the technology of network slicing and virtualization in 5G networks, see e.g. Afolabi et al. (2018).

With the network slicing scheme, transmission of warning signals is free of queuing delay, i.e., $\tau_q=0$, yet 5G networks also induce delay even at their fastest mode. Reports from the operational 5G infrastructures suggest the latency of $5-15ms$ for the fastest data transmission that is consistently achieved at the application level. Denote the latency of the fastest slice by τ_f. Hence, if k is the time instance a danger is detected by vehicle j, the warning signal will be received by the vehicle i at $k+\tau_{ul}+\tau_f+\tau_{dl}$.

4. PERFORMANCE ANALYSIS

We analyze the performance of the add-on safety features for the described communication scenarios on two critical parameters, *longitudinal slip ratio* and *stopping distance*, that represent aspects of safety. The stopping distance is the total traveled distance between the time that the braking system is activated until the vehicle is at standstill. Let a danger be detected by the vehicle j at a time k. The vehicle i is informed about the danger at time-step $k+r$, and r varies depending on the selected communication scenario. For the case that no V2I communication exists (Sec. 3.1), we have $r=\lceil\frac{RT}{T_s}\rceil$, where the ceiling operator is used to comply with the time-slotted framework of network operations. When employing the scenario of LTE BS without scheduling (Sec. 3.2), and assuming constant τ_{ul} and τ_{dl}, we have $r=\lceil\frac{\tau_{ul}+\tau_q+\tau_{dl}}{T_s}\rceil$ which is a function of τ_q that varies depending on the real-time queue length, arriving traffic at the BS, and the service bandwidth. For the 5G-supported BS enabled with network slicing (Sec. 3.3), vehicle i receives the warning signal with total latency of $r=\lceil\frac{\tau_{ul}+\tau_f+\tau_{dl}}{T_s}\rceil$. Denoting the time that vehicle i comes at complete standstill by $\bar{k}$, the stopping distance is the distance traveled by vehicle i during the interval $[k+r,\bar{k}]$.

Longitudinal slip ratio for vehicle i, denoted by κ_k^i, determines the tire slip in contact with road surface in longitudinal direction. As vehicles are equipped with ABS, which modulates the brake forces around the saturation region, we employ a linear model of slip ratio, as $\kappa_k^i=\frac{f_k^i}{C_i}$, where f_k^i denotes the longitudinal tire forces of vehicle i at time-step k and C_i is longitudinal tire stiffness. Assuming uniform normal load distribution and neglecting the load transfer and lateral effects of the control signal u_k^i, we have from the Newton's second law that $u_k^i=\frac{f_k^i}{M_i}$, with M_i the effective mass of the vehicle i. Therefore, we obtain the slip-acceleration relation, for vehicle i at time-step k, as

$$u_k^i=\frac{C_i}{M_i}\kappa_k^i. \tag{7}$$

It is desired that the vehicle i is at complete stop within a safe distance from vehicle j with smooth deceleration to avoid high slip and loss of maneuverability. It should be noted that, equality (7) is valid for low slip ratio. As ADS and vehicles are ABS-equipped, tire forces are kept around the saturation region to avoid high slip ratio, thus with this assumption, linear expression (7) remains valid.

Control input u_k^i represents the deceleration applied to vehicle through braking, and we are interested in finding the maximum deceleration during the stopping time (the infinity norm of the sequence of control inputs during the braking process.). From the moment that the ABS

is activated, it takes a short time, so called *pressure build-up time* (denoted by τ_p), till the maximum deceleration is reached. For the advanced braking technologies, τ_p is significantly short. For the ease of analyses, we assume that the maximum deceleration, when reached, remains constant till the vehicle comes to the complete standstill.

Assume that vehicle i has the speed v^{xi}_{k+r} when informed about a danger detected by vehicle j. In the presence of the event-based add-on safety, $\theta^i_{k+r}=1$ and add-on safety features are activated at time $k+r$ until $\bar{k}$. Total braking time of vehicle i is $\bar{k}-k-r$. As deceleration is constant after τ_p, and $\theta^i_t=1$, $\forall t\in[k+r,\bar{k}]$, the maximum deceleration of vehicle i during the braking process is obtained as

$$\begin{aligned}|u^i_{\max}| = |u^i_t|_\infty &= \max_{t\in[k+r,\bar{k}]}|u^i_t| \\ &= |-(\bar{c}^p_{ij}+\Delta c^p_i)(p^i_{\bar{k}-\tau_\epsilon}-p^j_{\bar{k}-\tau_\epsilon})- \\ &\quad (\bar{c}^v_{ij}+\Delta c^v_i)(v^{xi}_{\bar{k}-\tau_\epsilon}-v^{xj}_{\bar{k}-\tau_\epsilon})-c^p_0\,p^i_{\bar{k}-\tau_\epsilon}-c^v_0\,v^{xi}_{\bar{k}-\tau_\epsilon}|\end{aligned} \tag{8}$$

where, $\bar{k}-\tau_\epsilon$ is an infinitesimal moment before the time $\bar{k}$ ($\tau_\epsilon\approx 0$), when the maximum deceleration begins to reduce. The resulting maximum slip ratio during the time interval $[k+r+\tau_p,\bar{k}-\tau_\epsilon]$, can be obtained from (7) and (8), as

$$\kappa^i_{\max}=\frac{M_i}{C_i}|u^i_{\max}|, \tag{9}$$

and, $\kappa^i_{\max}$ is the maximum slip determined by the ABS.

4.1 Tuning safety parameters: desired maximum slip ratio

The add-on safety parameters $\Delta c^p_i, \Delta c^v_i$ are generally designed based on the safe distance with front vehicle and in order to maintain smooth deceleration that leads to low slip ratio and high maneuverability of the following vehicle. To have a meaningful comparison, first we discuss safety in form of final relative distance of the vehicles when they are at complete standstill, while Δc^p_i and Δc^v_i are adjusted such that slip ratio dose not exceed a desired value, denoted by $\bar{\kappa}^i_{\max}$. Hence, considering $\tau_\epsilon\approx 0$ for the ease of derivations, the following inequality is desired:

$$\frac{M_i}{C_i}|u^i_{\max}|\le\bar{\kappa}^i_{\max}. \tag{10}$$

We intuitively assume that the vehicle j, that has detected the danger before vehicle i, had already come to standstill at $\bar{k}$, i.e., $v^{xj}_{\bar{k}}=0$. Moreover, assuming τ_p is significantly short, we presume $v^{xi}_{k+r}\approx v^{xi}_{k+r+\tau_p}$. Since the maximum deceleration is constant during $[k+r+\tau_p,\bar{k}]$, we employ the quadratic equation of motion to compute the distance traveled by vehicle i during the mentioned interval, as

$$\begin{aligned}p^i_{\bar{k}} &= p^i_{k+r+\tau_p}+v^{xi}_{k+r+\tau_p}(\bar{k}-k-r-\tau_p) \\ &\quad+\frac{1}{2}u^i_{\max}(\bar{k}-k-r-\tau_p)^2.\end{aligned} \tag{11}$$

From (8), (10) and (11), and knowing $v^{xj}_{\bar{k}}=0$, the relative distance between two vehicles at $\bar{k}$ becomes

$$\begin{aligned}p^i_{\bar{k}}-p^j_{\bar{k}} &\le \frac{C_i\bar{\kappa}^i_{\max}}{M_i(\bar{c}^p_{ij}+\Delta c^p_i)}\left(1+\frac{(\bar{k}-k-r-\tau_p)^2}{2}\right) \\ &\quad-\frac{c^p_0\left(p^i_{k+r+\tau_p}+v^{xi}_{k+r+\tau_p}(\bar{k}-k-r-\tau_p)\right)}{\bar{c}^p_{ij}+\Delta c^p_i}.\end{aligned} \tag{12}$$

It can be seen from (12) that, under the maximum slip ratio constraint, the upper-bound on the standstill distance between two vehicles depends on r and Δc^p_i. The first parameter is determined by the choice of the communication scenario, and Δc^p_i is the event-triggered adjustment on the control input to augment the safety margin (relative distance). If no road-side communication exists, then we have $r=\lceil\frac{RT}{T_s}\rceil$, and $\Delta c^p_i=0$ which leads to a lower value for the right side of the inequality (12), i.e., in the absence of V2I-I2V communication, the vehicles are more prone to collide. Lower r increases the final relative distance. Hence, 5G with network slicing is superior to non-scheduled LTE as, first, high data rate traffic will not affect transmission of emergency signals, and second, queuing delay is removed.

Increasing Δc^p_i, that essentially leads to higher deceleration, also increases the final relative distance. However, we should note that, we are not allowed to increase Δc^p_i freely, as increasing it increases the slip ratio as well. At some point, increasing Δc^p_i will not increase deceleration due to ABS that keeps tire forces at maximum around the saturation region. It is concluded that, road-side communication clearly enhances safety margins, while between the two described communication schemes with infrastructure, 5G generally outperforms LTE as latency is at minimum.

The expression (12) does not guarantee that the vehicles never collide (i.e. $p^i_{\bar{k}}-p^j_{\bar{k}}\le 0$) for all values of $p^i_{k+r+\tau_p}$ and $v^{xi}_{k+r+\tau_p}$ and for any constants $C_i, M_i, \bar{c}^p_{ij}$ and $\kappa^i_{\max}$. We will see in the next section that even in the presence of add-on safety mechanism, if the vehicles initial speeds are high and their relative initial distance is short, then avoiding collision may not happen. However, shorter r and appropriate tuning of Δc^p_i increase the reaction time and the maximum deceleration to stop the vehicle in time. Moreover, shorter r results in farther back $p^i_{k+r+\tau_p}$ which increases the relative distance $p^i_{\bar{k}}-p^j_{\bar{k}}$, according to (12) [2].

4.2 Desired minimum relative distance

Now, consider that a minimum standstill relative distance between the vehicles i and j, denoted by $p^i_{\bar{k}}-p^j_{\bar{k}}\le p^{ij}_f$, is desired. Note that for a safe setup, p^{ij}_f must be negative. Having this, together with (8) and (11), we obtain

$$\begin{aligned}u^i_{\bar{k}} &\ge -\frac{|p^{ij}_f|\left(\bar{c}^p_{ij}+\Delta c^p_i\right)}{1+\frac{(\bar{k}-k-r-\tau_p)^2}{2}} \\ &\quad+\frac{c^p_0\left(p^i_{k+r+\tau_p}+v^{xi}_{k+r+\tau_p}(\bar{k}-k-r-\tau_p)\right)}{1+\frac{(\bar{k}-k-r-\tau_p)^2}{2}}.\end{aligned} \tag{13}$$

According to (13), for a desired p^{ij}_f, the maximum deceleration is a function of r and Δc^p_i. Similar to the Section 4.1, shorter r decreases the maximum required deceleration $u^i_{\bar{k}}$ to stop the two vehicles with the distance of p^{ij}_f. In the absence of the add-on safety mechanism, $\Delta c^p_i=0$ which results in higher deceleration. Having the event-triggered safety mechanism, we can decrease the maximum required deceleration by increasing Δc^p_i to stop the vehicles at the distance of p^{ij}_f. It can be deduced from (13) that, the greater the p^{ij}_f and v^{xi}_{k+r} are at $k+r$, the higher the

[2] We can repeat above discussions for relative velocity between the two vehicles, where we omit the details for the purpose of brevity.

deceleration is required. Nevertheless, to guarantee maneuverability, the maximum deceleration cannot be set too high as it leads to large slip ratio, i.e., $|u_k^i| \leq |u_{\max}^i|$. Hence, not any given p_f^{ij} is feasible, as the required maximum deceleration may not be realized by the ADS as the ABS does not allow the slip ratio to go beyond the safe region.

5. RESULTS AND DISCUSSIONS

Sudden changes in the path planning or vehicle formation control strategies in vehicle's dynamic stabilization programs leads to harsh brake (or throttle) actuation. As discussed in Sec. 2, high slip ratio originated by such harsh brake or acceleration requests results in considerable drop in lateral tire forces, thus makes vehicle more prone to instability. This section studies the advantages of utilizing the add-on safety mechanism to reduce high-slip scenarios by timely braking for two different driving cases. Validation has been done through software simulations in *CarSim*, which is a system-level high-fidelity vehicle dynamics simulator. The relative position and speed signals are available through radar and vision systems in the current driving systems. The ABS, as an inherent part of ADS and ADAS systems, is used in simulations. This supports the linear tire force assumption in Sec. 4.

The scenarios without V2I-I2V, non-scheduled LTE-based, and 5G-supported slicing-enabled communications, are denoted by NC, V2I, and SV2I, respectively. In simulations, vehicles are identical with mass $M = 1580$ kg, effective tire radius $R_e = 0.30$ m, and wheel base $W_b = 2.34$ m; constant and additive relative position and velocity gains are $\bar{c}_{ij}^p = 0.1, \bar{c}_{ij}^v = 0.23$ and $\Delta c_i^p = 0.04, \Delta c_i^v = 0.11$ for all vehicles; adjusting gains are $\bar{c}_0^p = 0.08, \bar{c}_0^v = 0.05$ obtained by several experiments in normal driving and at the edge of handling scenarios; the desired relative distance at standstill between two vehicles' centers of gravity is 10 m; and the longitudinal acceleration noise is zero-mean with the variance of 0.2m/s^2. It should also be mentioned that optimization on (constant and additive) control parameters is challenging and is out of scope of this work due to not having a global cost function, coupling with combined-slip tire forces, vertical forces at each corner, and uncertainties on model parameters. The longitudinal slip ratio $\kappa_l = \frac{R_e\omega_l - v^{xi}}{\max\{R_e\omega_l, v^{xi}\}}$ at a (font/rear) axles l of vehicle i, with R_e as the effective radius of the tyre, and ω_l as the average wheel speed at the axles l, is an indicator of healthy brake scenarios due to its correlation with the longitudinal tire forces; it is monitored in simulations.

In the first case (Case 1), a longitudinal deceleration scenario, due to a danger incidence in front of the lead vehicle j, is simulated and the responses (slip ratio and longitudinal speed/acceleration) of the behind vehicle i are demonstrated. The initial speed of vehicles j and i are 80 and 95 kph, respectively. The front vehicle's ADAS activates its brakes at $t = 0$, due to a danger, and the reaction time is assumed to be 0.7 s. The effect of communication is compared for non-scheduled (V2I) and 5G-supported slicing-enabled (SV2I) scenarios with $\tau_{ul} + \tau_{dl} = 0.015$ s. The queuing delay τ_q is realized from an exponential distribution with mean 0.05 s and variance 0.015 ms. The 5G network induces latency τ_f selected from a uniform distribution over the interval $[0.005, 0.015]$ s, for the fastest network slice. The measured longitudinal speed and acceleration for vehicles i and j are shown in Fig. 3.

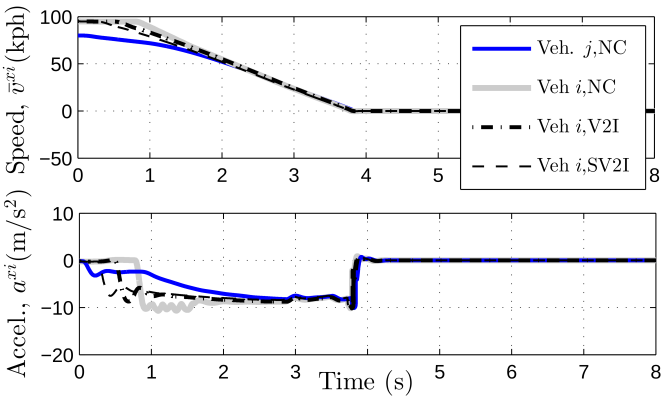

Fig. 3. Speed and acceleration profiles (measured) for vehicles i and j (blue) for NC, V2I, and SV2I scenarios

Fig. 3 shows that the front vehicle j has mild deceleration, but the measured acceleration for vehicle i quickly reaches to the capacity of the dry road (almost 10 m/s^2) to maintain desired spacing and stop effectively for NC scenario. This results in high slips and activation of the ABS (and consequent slip ratio oscillations) for NC scenario to modulate brake actuation around the longitudinal tire forces' saturation region (around slip ratio 22% on dry road); this is demonstrated in Fig. 4, in which longitudinal slip ratios for the front and rear axles of vehicle i is compared for NC, V2I, and SV2I communication scenarios in Case 1. Fig. 4 also shows that SV2I leads to the lowest slip ratio for this driving scenario, thus facilitates better maneuverability in case of sudden cornering/lane-change request by the driver or ADS. The minor difference between the slip ratios on front and rear tires are due to load transfer during brake, which is harsher for NC, that reduces longitudinal force capacity on rear tires, thus increases rear slip ratios.

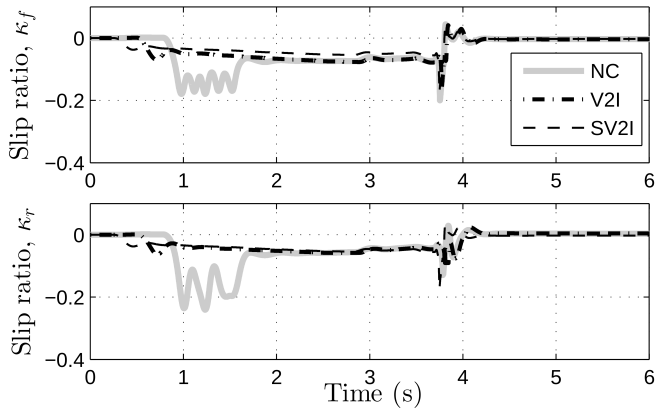

Fig. 4. Front and rear tires slip ratios of vehicle i – Case 1

To evaluate the performance of the add-on safety in harsher scenarios, in terms of maintaining the safe distance between vehicles, Case 2 is simulated. In this case, the test setup and vehicles are similar to Case 1, but the initial speeds of vehicles j and i are 85 and 110 kph, respectively. To show the effectiveness of three communication scenarios (NC, V2I, SV2I) in such harsh maneuver, the requested deceleration by the closed-loop system (2) and the measured one are shown in Fig. 5 for vehicle i. In Case

2, NC shows the largest deceleration request, which is not achievable due to the road-tire force capacity, thus, leads to brake modulation by the ABS around the saturation point to use the maximum attainable deceleration. However, the control system can not maintain the safe distance between two vehicles as can be seen from Fig. 5 (top), in which longitudinal position trajectories for both vehicles intersects at about 3.5 s and we observe collision. Longitudinal slip for Case 2 simulations are shown in Fig. 6, in which NC leads to large slips during long ABS activation.

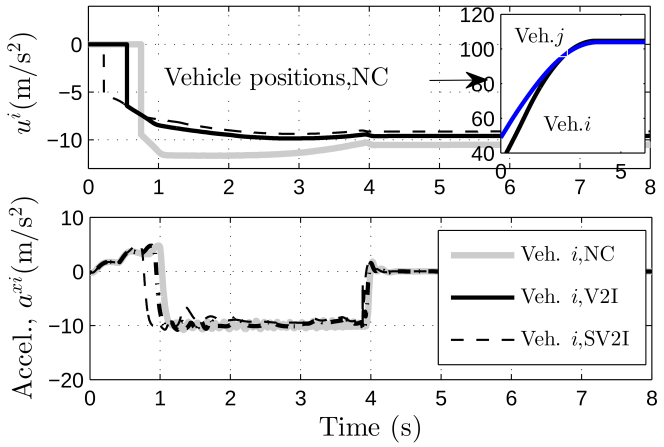

Fig. 5. Control inputs and measured accelerations for NC, V2I, and SV2I scenarios

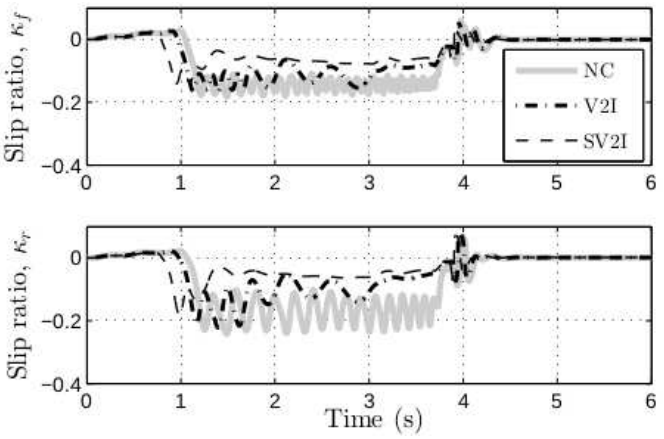

Fig. 6. Front/rear tyres' slip ratio for vehicle i in Case 2

In contrast, SV2I maintains longitudinal slip around 7%, which is convenient in terms of proactive and mild brake involvement, and also keeps the safe distance between two vehicles; the test with V2I also shows lower slip ratio, when compared with NC, which confirms effectiveness of V2I-based add-on safety mechanism for reducing longitudinal slip and maintaining safe distance between the vehicles.

6. CONCLUSION

In this paper, we propose an event-triggered safety mechanism that aims, together with the ADS system, to enhance the controllability of connected vehicles upon occurrence of on-road unexpected dangers. Using road-side infrastructure, warnings can be exchanged faster among the vehicles, activating the add-on safety features sooner. The control input is adjusted to avoid the danger safely, i.e. to avoid collision with smooth braking not to lose maneuverability. We study two wireless technologies to support communication between the vehicles and the base stations, the LTE and the 5G schemes, and compare the resulting performance on the vehicles safety margins.

REFERENCES

Afolabi, I., Taleb, T., Samdanis, K., Ksentini, A., and Flinck, H. (2018). Network slicing and softwarization: A survey on principles, enabling technologies and solutions. *IEEE Comm. Surveys Tut.*, 20(3), 2429–2453.

Bengler, K., Dietmayer, K., Farber, B., Maurer, M., Stiller, C., and Winner, H. (2014). Three decades of driver assistance systems: Review and future perspectives. *IEEE Intelligent Transportation Systems Mag.*, 6(4), 6–22.

Campolo, C., Molinaro, A., Iera, A., and Menichella, F. (2017). 5g network slicing for vehicle-to-everything services. *IEEE Wireless Communications*, 24(6), 38–45.

Chang, J. and et al. (2015). Estimated benefits of connected vehicle applications: dynamic mobility applications, AERIS, V2I safety, and road weather management applications. Technical report, US Transportation Dept.

Hung, S.C., Zhang, X., Festag, A., Chen, K.C., and Fettweis, G.P. (2019). Vehicle-centric network association in heterogeneous vehicle-to-vehicle networks. *IEEE Transactions on Vehicular Tech.*, 68(6), 5981–5996.

Ito, Y., Kamal, S., Yoshimura, T., and Azuma, S.i. (2018). Coordination of connected vehicles on merging roads using pseudo-perturbation-based broadcast control. *IEEE Transactions on Intelligent Transportation Systems*, 20(9), 3496–3512.

Krauss, D. and Olson, P. (2015). *Forensic Aspects of Driver Perception and Response*. Lawyers & Judges Publishing Company.

Linsenmayer, S., Dimarogonas, D.V., and Allgöwer, F. (2017). Event-based vehicle coordination using nonlinear unidirectional controllers. *IEEE Transactions on Control of Network Systems*, 5(4), 1575–1584.

Lu, N., Cheng, N., Zhang, N., Shen, X., and Mark, J.W. (2014). Connected vehicles: Solutions and challenges. *IEEE Internet of Things Journal*, 1(4), 289–299.

Lucena, J.O., Ameigeiras, P., Lopez, D., Ramos-Munoz, J., Lorca, J., and Folgueira, J. (2017). Network slicing for 5g with sdn/nfv: Concepts, architectures, and challenges. *IEEE Communications Magazine*, 55(5), 80–87.

Mamduhi, M.H., Baras, J.S., Johansson, K.H., and Hirche, S. (2018). State-dependent data queuing in shared-resource networked control systems. In *2018 IEEE Conference on Decision and Control (CDC)*, 1731–1737.

Molina, E. and Jacob, E. (2018). Software-defined networking in cyber-physical systems: A survey. *Computers and Electrical Engineering*, 66, 407–419.

Neely, M.J. (2010). *Stochastic Network Optimization with Application to Communication and Queueing Systems*. Morgan and Claypool Publishers.

Öncü, S., Ploeg, J., Van de Wouw, N., and Nijmeijer, H. (2014). Cooperative adaptive cruise control: Network-aware analysis of string stability. *IEEE Transactions on Intelligent Transportation Systems*, 15(4), 1527–1537.

Selmanaj, D., Corno, M., Panzani, G., and Savaresi, S.M. (2017). Vehicle sideslip estimation: A kinematic based approach. *Control Engineering Practice*, 67, 1–12.

Tegling, E. (2018). *Fundamental Limitations of Distributed Feedback Control in Large-Scale Networks*. Ph.D. thesis, KTH Royal Institute of Technology.